NUCLEATION OF THE SUPERSATURATED GLYCERIN VAPOR IN THE VICINITY OF MELTING POINT

M.P. Anisimov, A.G. Nasibulin, and S.D. Shandakova

Institute of Atmospheric Optics,
Siberian Branch of the Russian Academy of Sciences, Tomsk
Received January 26, 1996

In this paper we study experimentally the nucleation rate of glycerin vapor in the nucleation temperature interval including the vicinity of the melting point. Influence of melting on the nucleation rate has been revealed in this study. These facts should be taken into account in the theory of nucleation.

INTRODUCTION

Optical properties of the atmosphere are governed by its gas and aerosol composition.[1] The aerosol composition, in its turn, depends on the dynamics of atmospheric aerosol which is conditioned by the processes of coagulation, vaporization, condensation, nucleation, and sedimentation. Among the above processes, the nucleation is very important but most poorly known. In some papers (see, for example, Ref. 2), influence of nucleation on the dynamics of atmospheric aerosol has been noticed. However, modern models of atmospheric aerosol are far from a prompt account for it.

To reach some progress in this field, it is of fundamental importance and great urgency to find new details in the mechanism and to make more correct the axiomatics and assumptions of the nucleation theory. In order to achieve agreement between the results on nucleation rate measured using different experimental techniques and to refine the axiomatics of the nucleation theory, it was decided recently on the International Workshop on Nucleation (Prague, 1995)[3] to measure the pentanol nucleation rate under the same conditions for all measurement techniques. In addition to matching the results obtained by different methods, the authors of this paper believe studying the influence of change of the temperature dependence of condensed phase chemopotential on the nucleation rate isotherms to be quite appropriate. This is possible at the nucleation temperature in the vicinity of the phase transition, for example, melting. Glycerin is suitable for such experiments.

INSTRUMENTATION

In this study we used an automated experimental setup close, in principles of operation, to that described in Ref. 4. This setup provides a possibility of determining the nucleation rate as a function of degree of supersaturation of substances under study at different pressures of the carrier gas.

An aerosol generator for studying the spontaneous nucleation of vapors in a gas medium comprises hot and cold thermostats *5* (see Fig. 1). Copper parts of the thermostats are chrome-plated. The hot thermostat is a 120 mm-long copper tube with an outer diameter of 50 mm and wall thickness of 18 mm. At its outer surface a heater is installed. A precision thermoregulator keeps the thermostat temperature accurate to ±0.1° within the range 20−200°C. The temperature was controlled and measured with a copper-constantan thermocouple. The thermostat was filled with an inert chromatographic carrier (INZ-600, granulation of 0.5−1 mm). A carrier, annealed in the flowing helium atmosphere, was then impregnated with 20 wt% of a substance under study. A grid confines a carrier to the thermostat.

A pure inert carrier gas (content of the basic matter no less than 99.99%) flows from a bottle *1* through a filter *2*, a measurer and a gas flow rate regulator *3* and *4* into the thermostat *5*, where it flows through a chromatographic carrier *A* (Fig. 1) and saturates with vapors of the substance under study. The rate profile of a gas saturated with vapors becomes parabolic at the temperature of saturation in the part *B* of the thermostat. It is 40 mm long and 8 mm in diameter. Then the mixture comes to a cold tube *C*. A reducer between *B* and *C* is 8 mm long. The tube *C* keeps constant temperature with the MK70 cryostat accurate to 0.1°. Gas volumetric flow rates were reduced to a normal pressure and temperature of 20°C. An absolute error in measuring the gas flow rate was below 1.0%.

The concentration of aerosol generated was measured with an aerosol particle counter *6*. A programmed control over the time of counting improves the statistics in the region of small (up to 10^2 cm^{-3} s^{-1}) nucleation rates as compared to the previous counter design.[4] Our experience in the use of the scheme with enlargement of particles in a flow of slightly supersaturated gas (including the experiments when TSI counter has been used) shows that, at enlargement, particles can appear as a result of binary nucleation. To detect particles, foreign for the process under study, is

a very complicated problem. Therefore we believe it principally important to use a highly-sensitive laser counter allowing one to have a counter volume only 1–2 mm below the end of the output tube of an aerosol generator. It should be noted that at low nucleation rates our counter counts all particles rather than their fraction, as is usually accepted. As the concentration increases, the counter changes the mode of operation to the common mode of counting some known fraction of particles. The fraction of particles counted is determined by the calibration to the readouts of an absolute counter in the region of its normal operation. In our experiments the fraction of particles counted was less than 0.01.

The gas pressure in the condenser and the aerosol counter was the same and kept constant during one experiment. Information from sensors was transported to a personal computer for its further processing.
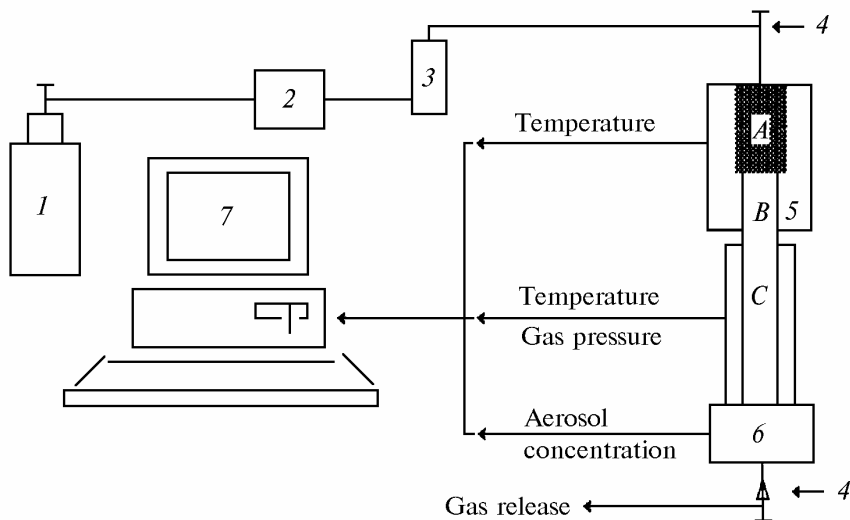

FIG. 1. *Block diagram of the experimental setup: a bottle with an inert gas 1, a filter 2, a gas flow rate meter 3, a regulator of gas flow rate and pressure 4, an aerosol generator 5, a counter of aerosol particles 6, and a personal computer 7.*

CALCULATION OF THE VAPOR SUPERSATURATION AND DETERMINATION OF THE NUCLEATION RATE

To determine the vapor supersaturation in the condenser, the equations of heat–and–mass exchange should be solved for a laminar stationary axisymmetric vapor–gas flow allowing for the viscosity. Stationary motion of the axisymmetric laminar flow of viscous gas can be described by the system of Navier–Stokes equations. In the cylindrical system of coordinates they have the following form[5]:

$$P = \rho R_0 T / m , \tag{1}$$

$$2\pi \int_0^R r\rho u \, dr = Q ; \tag{2}$$

$$\rho u \frac{\partial u}{\partial x} = -\frac{dP}{dx} + \frac{1}{r}\frac{\partial}{\partial r}\left(r\eta \frac{\partial u}{\partial r}\right) ; \tag{3}$$

$$\rho u C_p \frac{\partial T}{\partial x} = u \frac{dP}{dx} + \eta \left(\frac{\partial u}{\partial r}\right) + \frac{1}{r}\frac{\partial}{\partial r}\left(r\lambda \frac{\partial T}{\partial r}\right) , \tag{4}$$

where x is the coordinate of the axis of a cylindrical tube; r is the radial coordinate; u is the gas speed; T is the temperature; P is the pressure; ρ is the gas density;

η and λ are the gas dynamic viscosity and its thermal conductivity, respectively; C_p is the gas specific heat; R_0 is the universal gas constant; m is the gas molecular weight; R is the tube radius; Q is the gas mass flow rate.

Equations (1)–(4) have the following physical meaning: Eq. (1) is the equation of the ideal gas state; Eq. (2) is the continuity equation; Eq. (3) is the equation of conservation of momentum; Eq. (4) is the equation of the first law of thermodynamics.

In our case the motion of a carrier gas in cylindrical tube was described by Eqs. (1)–(4) with the following boundary conditions:

$$\left.\frac{\partial u}{\partial r}\right|_{r=0} = 0; \quad \left.\frac{\partial T}{\partial r}\right|_{r=0} = 0; \; u(R, x) = 0; \; T(R, x) = T_w(x),$$

$$T(r, 0) = T_0(r); \quad u(r, 0) = u_0(r), \tag{5}$$

where $T_w(x)$ is the preset temperature of the tube wall; $T_0(r)$ is the initial profile of the flow temperature at the tube entrance; $u_0(r)$ is that of the flow rate. When solving the problem we neglected the influence of minor gaseous constituents (vapor of the substance under study) on density, heat, heat content, viscosity, and thermal conductivity of the carrier gas. The

concentration ratio between the carrier gas and the substance under study was ~10^5 in our experiments. The carrier gas velocity and temperature fields were calculated by solving numerically the system of Navier–Stokes equations (1)–(4) with the boundary conditions (5) using the method of finite differences.

The error of solution of Eqs. (1)–(4) was estimated by comparing the exact analytical solution at ρ = const with the results of numerical solution.

In the case of ρ = const the system (1)–(4) is closed and at $x \to \infty$ and $T_w(x) = T_w$ = const it has the exact solution:

$$u = \frac{2Q}{R\pi^2\rho}\left(1 - \frac{r^2}{R^2}\right) ; \quad \frac{\partial P(x)}{\partial x} = -\frac{8Q\eta}{\pi\rho R^4} ;$$

$$P(x) = -8Q\eta/(\pi\rho R^4)x + P_0 ; \ T(r) = T_w = \text{const.} \quad (6)$$

A reference example was calculated at the following values of the parameters: $R = 0.4$ cm, $\eta = 2.095\cdot10^{-4}$ g/(s·cm); $P_0 = 1.013\cdot10^6$ dyn/cm^2; $\rho = 0{,}487\cdot10^{-2}$ g/cm^3; $Q = 0.0292$ g/s; $T_0 = 100$ K; $T_w = 293$ K; $\lambda = 2.22\cdot10^3$ cal/(cm·s·deg). The numerical calculations yield 23.9 cm/s for the gas speed, whereas the exact solution is 23.86 cm/s. Similarly for the pressure gradient: 0.1253 and 0.1250 dyn/cm^3, respectively. A comparative analysis of exact and approximate solutions of equations (1)–(4) describing gas motion gives the relative error of numerical calculations is below 0.5%.

Diffusion of vapors of the substance under study in a laminar stationary axisymmetrical flow of viscous gas, moving in a cylindrical tube, is described by the equation of molecular diffusion.[5] In the cylindrical system of coordinates it can be written as follows:

$$\rho u \frac{\partial C_i}{\partial x} = \frac{1}{r}\frac{\partial}{\partial r}\left(r\rho D_i \frac{\partial C_i}{\partial r}\right) . \quad (7)$$

This equation was solved by the method of finite differences. A boundary conditions have the following form:

$$C_i(R, x) = C_i^0(T_w(x)); \ \left.\frac{\partial C_i}{\partial r}\right|_{r=0} = 0; \ C_i(r, 0) = C_i^*(r),$$

where $C_i = \rho_i/\rho$ is the mass concentration of a vapor of the ith substance under study having the density ρ_i; D_i is the coefficient of molecular diffusion of the ith substance; $C_i^0(P, T_w(x))$ is the concentration of the saturated vapor of the ith substance on the tube wall (the tube walls are assumed to be covered with the substance under study); $C_i^*(r)$ is the initial profile of concentration of the ith substance at the tube entrance.

When estimating the accuracy of solution of the heat-and-mass exchange equations the flow speed profile at the tube entrance cross section is assumed to obey the Poiseuolle equation of viscosity.

Let the distribution of temperature and concentration of the vapor of the substance under study in the tube be written in the form

$$\tilde{T} = T_0(r^2x/R^3) + T_0 ;$$

$$\tilde{C}_i = C_i^*(r^2x/R^3) + C_i^* , \quad (8)$$

then

$$\tilde{T}(r, 0) = T_0; \ \left.\frac{\partial \tilde{T}}{\partial r}\right|_{r=0} = 0; \ \tilde{T}(R, x) = T_0 \frac{x}{R} + T_0, \quad (9)$$

$$\tilde{C}_i(r, 0) = C_i^*; \ \left.\frac{\partial \tilde{C}_i}{\partial r}\right|_{r=0} = 0; \ \tilde{C}_i(R, x) = C_i^* \frac{x}{R} + C_i^*. \quad (10)$$

Having substituted Eq. (8) into Eqs. (4) and (7), we derive

$$\rho u C_p \frac{\partial \tilde{T}}{\partial x} - u\frac{dP}{dx} - \eta\left(\frac{\partial u}{\partial r}\right)^2 - \frac{1}{r}\frac{\partial}{\partial r}\left(r\lambda\frac{\partial\tilde{T}}{\partial r}\right) =$$

$$\rho u C_p T_0 \frac{r^2}{R^3} + \frac{16\eta Q^2}{\pi^3 R^5\rho^2}\left(1 - \frac{r^2}{R^2}\right) + \frac{8\eta Q}{\pi^2 R^3\rho} - \frac{4T_0\lambda x}{R^3} ; \quad (11)$$

$$\rho u \frac{\partial \tilde{C}_i}{\partial x} - \frac{1}{r}\frac{\partial}{\partial r}\left(r\rho D_i \frac{\partial \tilde{C}_i}{\partial r}\right) = \rho C_i^* u \frac{r^2}{R^3} - \rho \frac{4C_i^* D_i\, x}{R^3} . \quad (12)$$

Expressions (8) are the exact solutions of Eqs. (4) and (7) with the right-hand sides of Eqs. (11) and (12) and boundary conditions (9) and (10) under the condition that

$$T_w(x) = T_0\,(x/R + 1) ;$$

$$C_i^0(x) = C_i^*\,(x/R + 1) . \quad (13)$$

To estimate the error of numerical solution of equations (4) and (7), the operators for calculating the right-hand sides of Eqs. (11) and (12) were added into the computer program. A comparison of the exact solution (8) with the results of numerical calculations has shown that the relative error of calculations does not exceed 0.5%.

In section B of the tube (see Fig. 1) the carrier gas contains the saturated vapor of the substance under study. Initial profiles of the carrier gas temperature and concentration of the vapor of the substance under study were assumed constant and independent of radius. The temperature T_w and the concentration C_i^0 on the wall in the section C of the tube (Fig. 1) were set constant. The tube wall served as a sink for the vapor in the condenser. A temperature change from T_0 to T_w at the B–C transition section $2R$ long was set as a smooth function of x. When solving the problem, the boundary conditions were as follows:

$$T(r, 0) = T_0 , \quad 0 \le r \le R ;$$

$$C_i(r, 0) = (kT_0)^{-1}\cdot10^{A - B/T_0}, \quad 0 \le r \le R ;$$

$$u(r, 0) = \begin{cases} u_0, & 0 \le r < R \\ 0 , & r = R \end{cases} ;$$

$$\left.\frac{\partial u}{\partial r}\right|_{r=0} = 0 ; \quad \left.\frac{\partial T}{\partial r}\right|_{r=0} = 0 ; \ u(0, x) = 0;$$

$$T(R, x) =$$

$$= \begin{cases} T_0, \ 0 \le x \le 8R \\ T_w + (T_0 - T_w)\cos^2[(\pi/4R)(x - 8R)], \ 8R < x < 10R; \\ T_w, \ 10R \le x \le 70R \end{cases}$$

$$C_i(R, x) = C_i^0(T(R, x)) = (1/kT(R, x)) \cdot 10^{A - B/T(R, x)};$$

$$\left.\frac{\partial C_i}{\partial r}\right|_{r = 0} = 0 \ ,$$

where A and B are the constants determining the elasticity of the saturated vapor of the working substance.[6]

Supersaturation $S(r, x)$ was defined by the distribution of temperature $T(r, x)$ and concentration $C_i(r, x)$ in the following way

$$S(R, x) = \frac{C_i(r, x)}{C_i^0(r, x)} = \frac{kT(r, x)C_i(r, x)}{10^{A - B/T(r, x)}} \ ,$$

where $C_i^0(r, x)$ is the concentration of the saturated vapor of the substance under study at the temperature $T(r, x)$.

The diffusion coefficient was calculated for the model of binary gas systems. An empirical dependence has the following form[5]:

$$D_i = \frac{0.001T^{1.75}\big[(1/M_1) + (1/M_2)\big]^{1/2}}{P\big[(\Sigma v)_1^{1/3} + (\Sigma v)_2^{1/3}\big]^2} \ ,$$

where P is the total pressure; M_1 and M_2 are the molecular masses of glycerin and SF_6, respectively; $(\Sigma v)_1$ and $(\Sigma v)_2$ are the molecular diffusion volumes of the components. The heat conductivity was calculated by the equation derived based on the data from Ref. 7:

$$\lambda = T^{1.75}(P\,a + b) + (P\,c + d) \ W/(m \cdot K) \ ,$$

where $a = -1.3454 \cdot 10^{-8}$; $b = 5.4658 \cdot 10^{-7}$; $c = 4.6048 \cdot 10^{-4}$, $d = 9.1314 \cdot 10^{-4}$, and the specific heat[11] $C_{SF_6} = 667.6 \, J/(kg \cdot K)$. Specific heat of SF_6 depends only slightly on temperature and pressure. The pressure of saturated glycerin vapors was calculated by the equation[6] $\log(P) = a - b/T$, where $a = 11.27423$ and $b = 4480.0$. The SF_6 gas constant[12] is $R_{SF_6} = 54.923 \, J/(kg \cdot s)$. The carrier gas density was calculated as

$$\rho = P/(R_{SF_6}\,T) \ .$$

The dynamic viscosity coefficient can be presented in the form[8]

$$\eta = [1/\pi d^2] \, (kTm/\pi)^{1/2} \ ,$$

where d is the diameter of a molecule.

The solutions for $T(r, x)$, $S(r, x)$, and $J(r, x)$ are shown respectively in Figs. 2, 3, and 4.

Maximum nucleation rate was found following the algorithm proposed in Ref. 9. To do this, one needs a theoretical expression for the nucleation rate. It is

obvious that the ratio of the maximum nucleation rate J_{theor}^{max} to the calculated number of aerosol particles produced by an aerosol generator per unit time $(N_{theor} = \int J_{theor}dv)$ is approximately equal to the corresponding ratio between the experimentally measured values, i.e.

$$\frac{J_{theor}^{max}}{\int J_{theor}\,dv} \cong \frac{J_{exp}^{max}}{N_{exp}} \ .$$

Approximate equality can be accounted for by the poorly developed theory. However, the use of theoretical values gives only slightly inaccurate value of the ratio, since poorly determined coefficients entering into the theoretical expression for nucleation rate are cancelled out practically exactly. This fact is supported by the comparison of theoretically calculated nucleation volume with the experimentally determined one. The expression for the maximum nucleation rate can be readily derived in the form

$$J_{exp}^{max} = \frac{N_{exp}J_{theor}^{max}}{\int J_{theor}\,dv} \ ,$$

where N_{exp} is the number of particles produced by an aerosol generator per unit time. If the similarity between the distributions of vapor concentration and the temperature holds (it is fulfilled in experiment), the maximum nucleation rate proves to be independent of the gas flow rate. This fact reduces the requirements to the accuracy of measuring the latter.
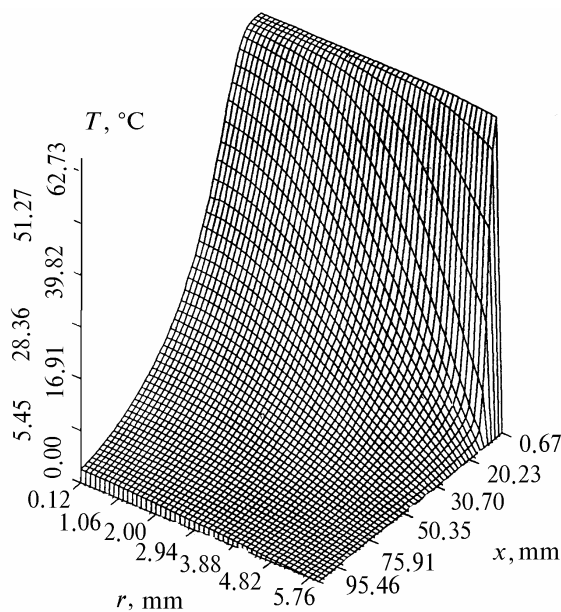

FIG. 2. Temperature distribution over a condenser: x is the coordinate along the tube axis and r is the radial coordinate.
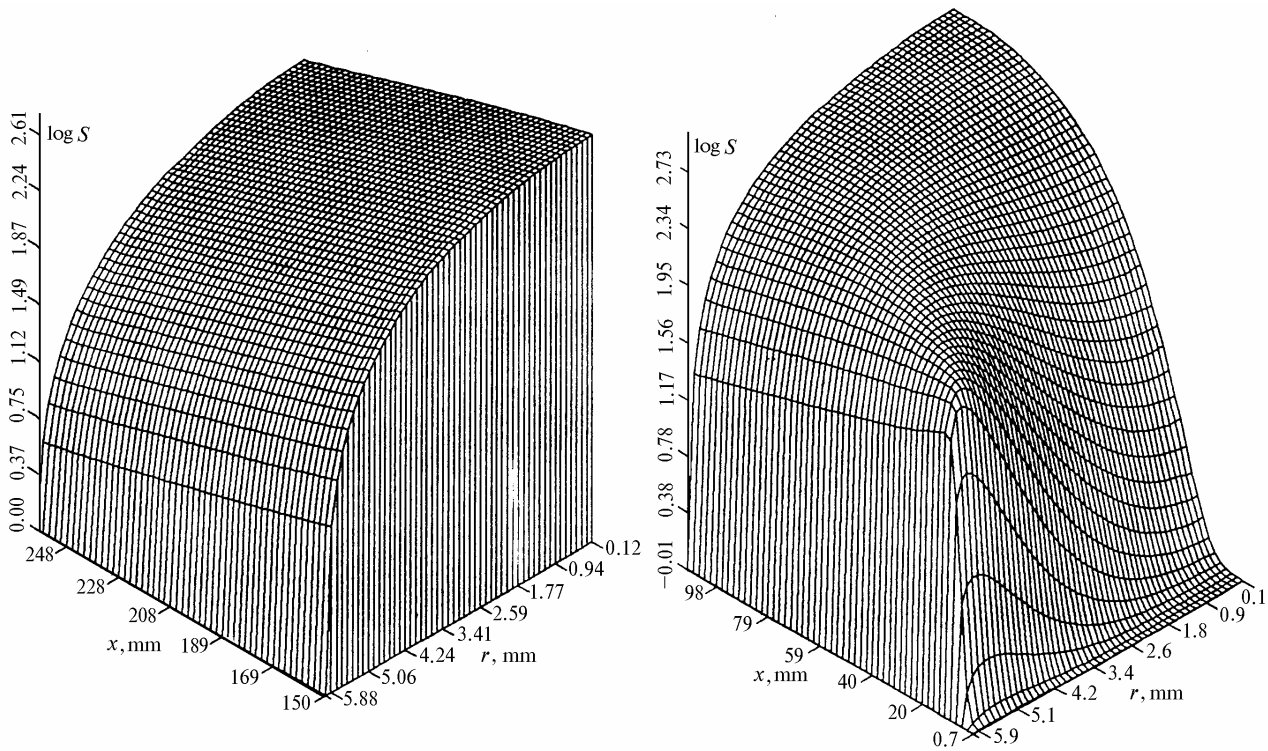
FIG. 3. Supersaturation distribution over a condenser: x is the coordinate along the tube axis and r is the radial coordinate.
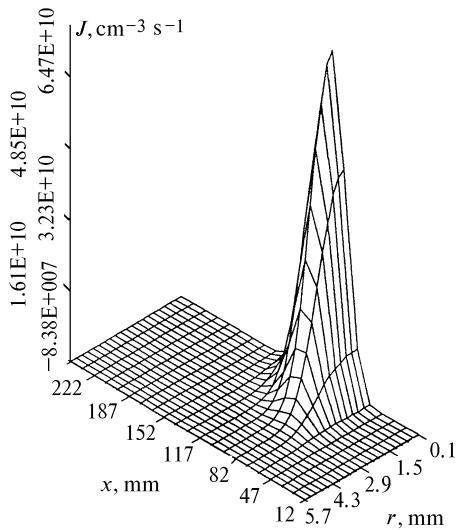

FIG. 4. Distribution of the rate of aerosol formation over a condenser: x is the coordinate along the tube axis and r is the radial coordinate.

EXPERIMENTAL RESULTS

Experimental dependences of $\log J$ on $\log S$ are shown in Fig. 5. The error of estimating the nucleation rate is a combination of the systematic and random errors of measuring the number of aerosol particles produced and the error of calculation of the nucleation volume. The absolute error of estimating the concentration of aerosol produced was no more than 20%.

The errors ΔD_i, $\Delta\lambda$, and $\Delta\eta$ were determined by the accuracy of the values D_i, λ, and η presented in Ref. 7, and they were about one per cent. The relative error of measuring the temperature and the pressure in our experiments was no more than 2%. The derivatives S and T of D_i, λ, η, P, and T_w were found by numerical differentiation. The total relative error of S and T calculation was about 5–8%. This error is mainly due to inaccuracy in determination of the thermophysical constants. Absolute error in estimating the nucleation volume did not exceed 40%. Therefore it can be derived that the nucleation rate was determined in our experiments accurate to ±0.5 of the order of magnitude.

DISCUSSION

As is evident from the qualitative analysis the change in the chemopotential of the condensed phase should have an effect on the nucleation rate of the vapor. In this case of the first-kind phase transition, the chemopotential may be a discontinuous function of temperature. Such its behavior is connected with a metastable state of the condensate. In the vicinity of the phase transition, the nucleation of both phases may occur. That is why the experimental curves of the nucleation rate are the sums of the rates of nucleation into different phase states of the condensate. It is quite probable that in the future an approach will be developed to estimation of the fractions of different phases.
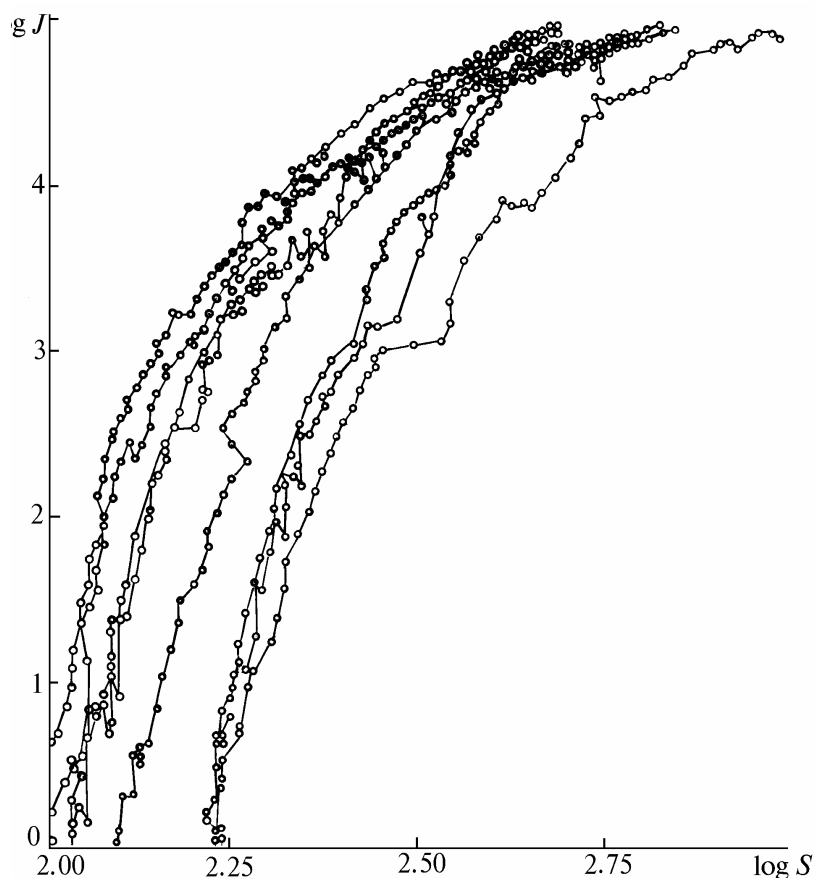
FIG. 5. Nucleation rate (J) of glycerin vapors in SF_6 as a function of supersaturation (S) at the nucleation temperature of 29.5, 26.5, 25, 23, 20, 18, 16.5, and 15°C (these values corresponds to the curves from left to right).
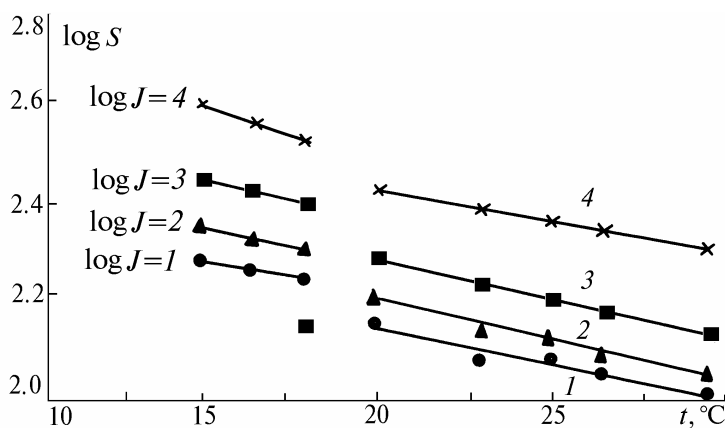

FIG. 6. Logarithm of glycerin vapor supersaturation as a function of nucleation temperature at fixed nucleation rates.

As follows from Ref. 10, the dependence of the vapor supersaturation on the nucleation temperature at the fixed rate contains information about the surface energy of critical centers of a new phase. A nonmonotonic form of the $S(T)$ dependence should be an indication of a nonmonotonic behavior of the surface energy of these centers.

Figure 6 shows $\log S$ as a function of the glycerin nucleation temperature at four different values of the nucleation rate ($\log J = 1, 2, 3,$ and 4). It can be seen that for all values this function is discontinuous. The discontinuity coincides with the temperature interval of glycerin melting. We do not present here intermediate cross sections since they can easily be obtained from the data presented above. The temperature corresponding to the points of discontinuity (or the transient zone) of $\log S$ grows as the nucleation rate increases. The change of the slope of $\ln S(T)$ at a fixed nucleation rate is

indicative of the anomalous temperature dependence of the surface energy of critical clusters and the influence of the first-kind phase transition in the condensate on the nucleation of supersaturated vapors.
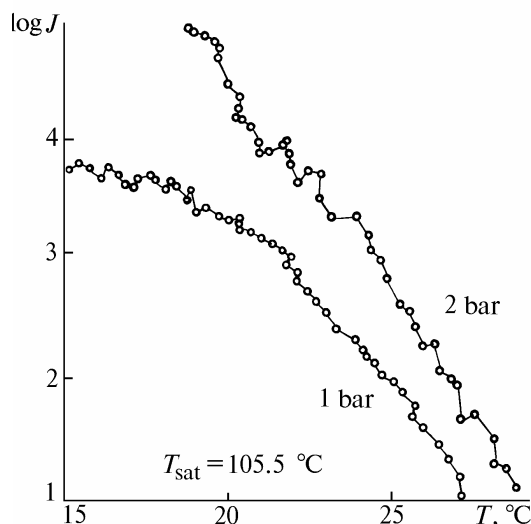

FIG. 7. Rate of isobaric nucleation against the nucleation temperature at the glycerin pressure corresponding to the saturation temperature: 105.5°C, and two different pressures (1 and 2 bar) of SF_6.

The dependence of the isobaric nucleation rate on the nucleation temperature at the glycerin pressure corresponding to the saturation temperature of 105.5°C as well as those at two different pressure (1 and 2 bar) of SF_6 is shown in Fig. 7. It can be seen from this figure that for the SF_6 pressure of 1 bar a discontinuity of the first derivative $d\log J/dt$ takes place at the temperature of 16°C, whereas at the pressure of 2 bar it occurs at 18°C. As known,[4] the value of this derivative is governed by the enthalpy of a phase formation. Here we observe a qualitatively correct growth of enthalpy with a jump that can be naturally assigned to the enthalpy of the condensate melting.

CONCLUSION

This paper dealt with the study of nucleation of a supersaturated vapor in the vicinity of the temperature of condensate melting. The influence of discontinuity of the temperature run of the condensate chemopotential upon the rate of aerosol formation has been discovered. Promising is the study in the region of phase transitions of the second kind and in the vicinity of the critical point (line or surface), as a particular case of phase transitions of the second kind. Preliminary results obtained in this work demonstrate the influence of the phase transition of the first kind (melting) on the nucleation of the supersaturated vapor. The atmospheric nucleation often occurs almost under conditions of water or water solutions freezing. Therefore, the study of model systems in the vicinity of phase transitions in the condensed state is promising for the theory of atmospheric heterogenic and heteromolecular nucleation.

REFERENCES

1. V.E. Zuev and G.M. Krekov, *Optical Models of the Atmosphere* (Gidrometeoizdat, Leningrad, 1988), 250 pp.
2. M.V. Panchenko and S.A. Terpugova, in: *Proc. of Ninth Annual Conference on Aerosols, Their Generation, Behaviour, and Applications,* Norwich, Great Britain (1995), pp. 163–175.
3. *Proc. of the International Workshop on Nucleation Experiments, State of the Art and Future Developments,* Czech Republic, Prague (1995), p. 25.
4. M.P. Anisimov, in: *Aerosols, Science, Industry, Health, and Environment: Proc. 3rd. Int. Aerosol Conf.,* Kyoto, Japan, Sept. 24–27, 1990 (Pergamon Press, Oxford etc., 1990), Vol. 1, pp. 146–150.
5. R. Reed, J. Prausnits, and T. Sherwood, *Properties of Gases and Liquids* [Russian translation] (Khimiya, Leningrad, 1982), 592 pp.
6. A.G. Amelin, *Theoretical Grounds of Fog Formation at Vapor Condensation* (Khimiya, Moscow, 1972), 304 pp.
7. N.V. Vargaftik, L.P. Filippov, A.A. Tarzimanov, and E.E. Totskii, *Handbook on Thermal Conductivity of Liquids and Gases* (Energoizdat, Moscow, 1990).
8. E.A. Melvin-Hews, *Physical Chemistry* [Russian translation] (Foreign Literature Press, Moscow, 1962), Vol. 1, 519 pp.
9. P.E. Wagner and M.P. Anisimov, J. Aerosol Sci. **24**, S103 (1993).
10. M.P. Anisimov and A.V. Taylakov, J. Aerosol Sci. **20**, No. 8, 1063–1066 (1989).
11. V.A. Rabinovich and Z.Ya. Khavin, *Concise Chemical Handbook* (Khimiya, Leningrad, 1991), 432 pp.
12. V.N. Zubarev, A.S. Kozlov, B.N. Kuznetsov, et al., *Thermophysical Properties of Practically Important Gases at High Temperature and Pressure* (Energoizdat, Moscow, 1989), 231 pp.